



Published in final edited form as:

*Biosens Bioelectron.* 2010 December 15; 26(4): 1297–1301. doi:10.1016/j.bios.2010.07.017.

## Carbon nanotubes-based chemiresistive immunosensor for small molecules: Detection of nitroaromatic explosives

Miso Park<sup>†</sup>, Lakshmi N Cella<sup>‡</sup>, Wilfred Chen<sup>†</sup>, Nosang V. Myung<sup>†</sup>, and Ashok Mulchandani<sup>†</sup>

<sup>†</sup> Department of Chemical and Environmental Engineering; University of California, Riverside, CA 92521, USA

<sup>‡</sup> Cell, Molecular and Developmental Biology Graduate Program; University of California, Riverside, CA 92521, USA

### Abstract

In recent years, there has been a growing focus on use of one-dimensional (1-D) nanostructures, such as carbon nanotubes and nanowires, as transducer elements for label-free chemiresistive/field-effect transistor biosensors as they provide label-free and high sensitivity detection. While research to-date has elucidated the power of carbon nanotubes- and other 1-D nanostructure- based field effect transistors immunosensors for large charged macromolecules such as proteins and viruses, their application to small uncharged or charged molecules has not been demonstrated. In this paper we report a single-walled carbon nanotubes (SWNTs)-based chemiresistive immunosensor for label-free, rapid, sensitive and selective detection of 2,4,6-trinitrotoluene (TNT), a small molecule. The newly developed immunosensor employed a displacement mode/format in which SWNTs network forming conduction channel of the sensor was first modified with trinitrophenyl (TNP), an analog of TNT, and then ligated with the anti-TNP single chain antibody. Upon exposure to TNT or its derivatives the bound antibodies were displaced producing a large change, several folds higher than the noise, in the resistance/conductance of SWNTs giving excellent limit of detection, sensitivity and selectivity. The sensor detected between 0.5 ppb and 5000 ppb TNT with good selectivity to other nitroaromatic explosives and demonstrated good accuracy for monitoring TNT in untreated environmental water matrix. We believe this new displacement format can be easily generalized to other one-dimensional nanostructure-based chemiresistive immuno/affinity-sensors for detecting small and/or uncharged molecules of interest in environmental monitoring and health care.

### Keywords

Carbon nanotubes; chemiresistor; field-effect transistor; label-free; immunosensor; explosives

### 1. Introduction

2,4,6-Trinitrotoluene (TNT) is a dual use compound that has found applications both for peaceful industrial and military/terrorist purposes. It is used as ammunition/explosive and in the manufacturing of dyes, plasticizers, herbicides, etc. Because of its persistence, traces of this harmful chemical can be found in soil and groundwater in the vicinity of manufacturing

Correspondence to: Ashok Mulchandani.

**Publisher's Disclaimer:** This is a PDF file of an unedited manuscript that has been accepted for publication. As a service to our customers we are providing this early version of the manuscript. The manuscript will undergo copyediting, typesetting, and review of the resulting proof before it is published in its final citable form. Please note that during the production process errors may be discovered which could affect the content, and all legal disclaimers that apply to the journal pertain.

plants and areas with past or current military activities for a long time. TNT contamination has a serious adverse effect on all life forms of our ecosystem (Pennington and Brannon, 2002; Shriver-Lake et al., 2002; Shriver-Lake et al., 1997). In humans, TNT can cause anemia, abnormal liver function, skin irritation and weakened immune system and it has been classified as a potential carcinogen by the U.S. Environmental Protection Agency (EPA) (Roberts et al., 1993). Therefore, there is a great need for on-site, rapid, reliable, inexpensive and sensitive detection of TNT in groundwater and soil. Various analytical methods, such as gas chromatography (GC), high performance liquid chromatography (HPLC), mass spectroscopy (MS), X-ray imaging have been utilized for monitoring TNT (Halasz et al., 2002; Walsh, 2001; Yinon and Zitrin, 1993). Although highly sensitive, these techniques require bulky and expensive analytical instruments, sample pretreatment and trained technicians, and cannot be field-deployed (Shankaran et al., 2005).

Immunosensor/affinity-biosensor is a promising technology that is rapidly gaining recognition as an important analytical tool for rapid, on-site/point-of-care trace level monitoring of complex biological and environmental samples. These sensing devices are constructed by combining the specificity/affinity of antibody-antigen reaction with the signal transducing and processing capability of competent electrical and/or optical components. The first generation immunosensors employed the sandwich format with radionuclide, enzyme, fluorophore or redox labeled secondary antibody for signal generation. The lack of an ideal label and the relatively slow speed of detection are the limitations of label-based immunosensors. The second generation immunosensors circumvent these shortcomings by directly measuring the physical changes induced by the formation of the complex such as refractive index using surface plasmon resonance (SPR), and mass by quartz crystal microbalance (QCM), and piezoelectric or surface acoustic wave (SAW) transducers (Elkind et al., 1999; Larsson et al., 2006; Shankaran et al., 2005).

One-dimensional (1-D) nanostructure based field-effect transistor (FET)/chemiresistor, with carbon nanotubes, silicon nanowires, conducting polymer nanowires, III-V semiconductor, metal oxide, etc is rapidly gaining recognition as a powerful transducer in label-free monitoring of antigen and antibody binding (Bangar et al., 2009; Wanekaya et al., 2006; Allen et al., 2007; Patolsky et al., 2006; Hangarter et al., 2010; Kim et al., 2007). Besides label-free detection, 1-D nano-FET/chemiresistor advantages include, extremely high sensitivity (potentially down to single molecule), ease of miniaturization, low power requirement and development of high density arrays that will allow simultaneous analysis of a range of different species in extremely small sample volume and reduce false negatives/positives due to massive redundancy. The resistance/conductance of these devices is extremely sensitive to any surface adsorption/perturbation and is a function of the analyte charge. Because of this charge dependence of the sensor sensitivity, successful demonstrations of 1-D nanostructure-based FET immunosensor have been limited to targets with large charges such as proteins, DNA, RNA, viruses, spores and cells. Thus the use of 1-D chemiresistor/FET immunosensor for highly sensitive and selective detection of small and/or weak-/un-charged molecules, important in environmental monitoring, such as TNT, and health care, remains a challenge.

The objective of this study is to develop, characterize and evaluate a 1-D nanostructure based chemiresistive immunosensor for label-free and highly sensitive detection of TNT, a small molecule. In order to achieve this goal, we developed a displacement mode/format nano-immunosensor (Fig. 1A) in which a network of single-walled carbon nanotubes (SWNTs) forming the conduction channel between the source and drain electrodes of the nano-chemiresistive was first modified with trinitrophenyl (TNP), an analog of the target analyte TNT, and then ligated with a highly charged anti-TNP single chain antibody (scAb). The introduction of the target analyte, TNT, that has a higher or comparable binding affinity

to anti-TNP scAb resulted in the displacement of the attached scAb producing a large change, several folds higher than the noise, in the nano- chemiresistive resistance/ conductance giving an excellent limit of detection sensitivity and selectivity. Using the displacement principle, we were able to detect 0.5 ppb to 5000 ppb TNT in buffer and also demonstrated the utility of the sensor for monitoring TNT in untreated water samples with adequate reliability.

## 2. Experimental

### 2.1. Reagents

2,4,6-trinitrophenyl (TNP) coupled with ovalbumin (OVA) was purchased from Biosearch Technologies (Novato, CA, USA). 2,4,6-trinitrotoluene (TNT), 1,3,5-trinitrobenzene (TNB), 2-amino-4,6-dinitrotoluene (2A-4,6-DNT), 2,4-dinitrotoluene (2,4-DNT), toluene, Tween 20, dimethyl formamide (DMF) and reagents for phosphate buffer (PB) were acquired from Sigma (St. Louis, MO, USA). HisBind resin for antibody purification was purchased from Novagen (Madison, WI, USA). Single-walled carbon nanotubes with high carboxylated functionality, sold under the trade name of P3-SWNT, were obtained from Carbon Solutions, Inc. (Riverside, CA, USA). Environmental water was sampled from run-off in Albuquerque area in New Mexico.

### 2.2. Preparation of single chain antibody (scAb)

*Escherichia coli* Tuner cells transformed with pMoPac16 harboring the anti-TNP scAb gene were grown overnight at 30 °C in terrific broth (TB) containing 2% glucose and 200 µg/mL ampicillin. Cells were transferred into a fresh medium without glucose and grown at 30 °C until the OD<sub>600</sub> was about one and induced with 1 mM IPTG for four hours at 25 °C. After pelleting, the cells were osmotically shocked and fractionated to recover the periplasmic fraction as described by Goldman et al. (2003). In brief, the pellet was suspended in 10 mL of 0.75 M sucrose in 0.1 M Tris (pH 7.5) to 50-fold original OD<sub>600</sub> and 20 mL of 1 mM EDTA was drip added followed by 2 mL of 0.5 M MgCl<sub>2</sub> to improve the efficiency of release of the cell periplasmic space. All the periplasmic fraction extraction steps were done on ice. The periplasmic fraction was then recovered by centrifugation at 30,000 g-force for 30 minutes and the anti-TNP scAb purified by affinity chromatography of polyhistidine-tag using HisBind Resin.

### 2.3. Sensor fabrication

Figure 1C shows the schematic of the immunosensor fabrication protocol. In brief, a uniformly dispersed and separated SWNTs suspension (without the formation of chemical bonds) was prepared by ultrasonication (power level 9) and centrifugation (10,000 rpm) a 25 µg SWNTs in 1 mL DMF for three different times (90, 60, 30 min for each cycle). 0.1 µL of the dispersed SWNTs were aligned across a pair of the 3 µm apart microfabricated gold electrodes by AC dielectrophoresis (DEP) by applying a 4 MHz (amplitude 0.366V p-p) AC field across the electrodes for a few seconds using a function generator (Wavetek, Alpharetta, GA, USA) followed by annealing at 300 °C for an hour under a continuous flow of 95% nitrogen gas mixed with 5% hydrogen. The SWNTs interconnects/channel of the chemiresistor was functionalized with TNP by incubating with 200 µL of TNP-OVA solution (1 mg/mL in PB) for overnight at room temperature, washed three times with PB followed by incubation with 0.1% Tween 20 (to block uncovered area on SWNTs to prevent non-specific binding). The samples were washed three times with PB, incubated with anti-TNP scAb solution (0.2 mg/mL in 200 µL buffer) for 3 hours and washed with PB three times.

## 2.4. Sensing measurements

The sensing protocol consisted of monitoring the initial resistance ( $R_0$ ) of the immunosensor fabricated above by measuring the source-drain current ( $I$ ) as a function of source-drain voltage ( $V$ ) from  $-1$  V to  $+1$  V using a HP 4155A (Agilent, Santa Clara, CA, USA) semiconductor parameter analyzer and taking the inverse of the slope of the I-V curve from  $-0.1$  V to  $+0.1$  V followed by incubation for 5 min at room temperature with different concentrations of analytes (TNT and derivatives) in buffer followed by washing three times with PB and recording the new resistance as before. Since TNT and other derivatives of TNT were provided in organic solvent, acetonitrile, phosphate buffer containing acetonitrile without any explosives was employed as a negative control. Various concentrations of TNT were spiked to the untreated environmental water sample for evaluating the utility of the sensor. All the I-V measurements were carried out in pH 7.2, 10 mM PB.

## 3. Results and discussion

SWNT-based chemiresistive sensors have utilized either a single SWNT or an ensemble/network of SWNTs as the conduction channel/gate bridging the source and drain electrodes. Because they can be prepared on a prefabricated micro-electrode by drop casting of a SWNTs suspension -- making the process simple, cost-effective and scalable -- we have chosen the SWNTs network platform for our work. The drop casting technique was combined with AC dielectrophoresis to assist in detangling SWNTs into small bundles and alignment/orientation of nanotubes perpendicular to the source and drain (Fig. 1B) to improve the device on-off characteristics (Lim et al., 2010) and annealing to improve contact between the nanotubes and gold electrodes.

SWNTs were modified with TNP, a TNT analog, non-covalently through the coupled protein, ovalbumin (OVA). Proteins can be physically adsorbed (non-covalently) strongly to carbon nanotubes through hydrophobic interaction (Azamian et al., 2002; Teker et al., 2005) while maintaining the electrical properties of SWNTs by protecting the carbon  $sp^2$  character and structure, critical for constructing high sensitivity sensor. Additionally, proteins can bind to gold surface through the cysteine group by forming Au-S bond. TNP-OVA functionalization of SWNT chemiresistive device was verified by monitoring the change in device resistance (inverse of the slope of I-V curves in Fig. 2). As shown, the resistance of the device increased upon the non-covalent immobilization of TNP-OVA (trace 2, Fig. 2) compared to the bare SWNTs (trace 1, Fig. 2). Subsequent incubation of the device with anti-TNP scAb produced an additional resistance increase (trace 3, Fig. 2). The resistance changes are attributed to the reduction in the charge carriers (holes) in the p-type semiconductor SWNT from an accumulation of negative charge and/or scattering potential as a result of TNP-OVA adsorption and scAb binding to TNP-OVA and modulation of work function difference between gold electrodes and SWNTs. To confirm that anti-TNP scAb was indeed binding to TNP and not OVA, binding of anti-TNP scAb to OVA functionalized SWNTs was investigated. No change in resistance (data not shown) was detected. As an additional verification of biosensor fabrication protocol, TNP-OVA functionalized SWNTs were incubated with fluorescein-labeled anti-TNP scAb, and the final product was observed under the fluorescence microscope. The presence of highly intense green fluorescence (Supplemental information Fig. S1) compared to negative control (SWNTs were coated with OVA alone) confirmed the successful functionalization of SWNTs by TNP and specificity of the anti-TNP scAb to TNP. Surface characterization of SWNTs by atomic force microscopy (AFM) observation also corroborated the successful modification of SWNTs. The shift of height distribution of SWNTs surface after TNP-OVA adsorption on bare carbon nanotubes indicated the adsorption of the analog conjugate on SWNTs (Supplemental information Fig. S2)

To examine the displacement principle of detection and the functionality of the immunosensor for TNT, I-V characteristics of the chemiresistive immunosensor after incubation with 5000 ng/mL TNT in PB with 0.5% acetonitrile for 5 min at room temperature, was measured. As shown in Fig. 2 (trace 4), the I-V reverted to that obtained for SWNTs with TNP-OVA. Similarly, there was a significant loss in the fluorescence intensity of the SWNTs+TNP-OVA+anti-TNP scAb-FITC (Supplemental information Fig. S1, Panel 2) when incubated with TNT (Supplemental information Fig. S1, Panel 3) compared to PB (Supplemental information Fig. S1, Panel 4). To confirm that the resistance modulation observed in the above investigation was from TNT and not acetonitrile, the biosensor response upon incubation with 5% acetonitrile in PB was investigated. There was no change in both the device resistance and fluorescence (data not shown). These results confirm the sensor response was a result of the highly specific competition between the surface attached TNP and free TNT for the anti-TNP scAb and the successful detection of TNT, an environmentally important small molecule, by the chemiresistive transducer using the displacement modality.

The concentration dependent I-V curves and the corresponding calibration plot for the displacement-based chemiresistive immunosensor in PB are presented in Figure 3. The response  $[(R - R_0)/(R_{scAb} - R_0)]$  where R is the resistance after exposure to the analyte,  $R_{scAb}$  is the resistance after binding of the antibody to TNP and  $R_0$  is the initial sensor resistance] was inversely proportional to TNT concentration in the solution over a range of 0.5 ng/mL to 5000 ng/mL. A sigmoidal calibration curve, which is typical for competitive immunoassay was observed. The  $IC_{50}$  was determined to be 26 ng/mL. These analytical characteristics are better compared to continuous flow immunosensors using the single chain antibody used in the present work (LOD = 1 ng/ml) (Goldman et al., 2003) and monoclonal antibody (LOD = 2.5 ng/ml) (Green et al., 2002) but using labels and comparable to a surface plasmon resonance immunosensor based on competitive immunoassay format using a monoclonal antibody (LOD = 1 ng/ml) (Shankaran et al., 2005).

Specificity/selectivity is critical for the successful measurement by a sensor. Figure 4 and Table 1 report the immunosensor calibration plots and  $IC_{50}$ , respectively, for 2,4-dinitrotoluene, 2 amino-4,6-dinitrotoluene, toluene, and 1,3,5-trinitrobenzene (TNB). The immunosensor had no selectivity against TNB (a high sensitivity and low  $IC_{50}$ ). This is not unexpected as TNB is structurally similar to the immunogen (TNP-OVA) used for generating the antibody used in this immunosensor. While this may appear to be a serious limitation of the sensor, it should be noted that TNB/TNP is neither an explosive nor TNT degradation product and therefore may not be present at TNT contaminated sites. On the other hand, the sensor had a near perfect/total discrimination against 2-4 dinitrotoluene and toluene. There was a moderate cross-reactivity to 2-amino, 4,6-dinitrotoluene. These results are in agreement with the continuous flow immunosensor reported by Goldman et al (2003).

The utility of the immunosensor for the analysis of environmental sample was investigated by using TNT spiked surface water sample from Albuquerque, NM, area without any pretreatment. The response of sensors upon incubation with environmental water sample spiked with three different concentrations of TNT was measured and the concentration was determined using the calibration plot in Fig. 3B. As shown in Table 2, the immunosensor displayed good accuracy with the recovery range from 80 to 110 %, establishing the utility of the sensor for detection of TNT in untreated environmental water samples. This indicates that the sensor is highly specific towards its target and it can be utilized for on-site monitoring with untreated water samples from the environment. The high correspondence between the values measured in buffer and environmental water sample is significantly better than the 50% reported between buffer and sea water (Green et al., 2002).

## 4. Conclusions

To summarize, a simple, rapid, highly sensitive and selective single-walled carbon nanotubes network chemiresistive immunosensor device for the label-free detection of 2,4,6-trinitrotoluene was developed, characterized and applied to environmental water samples. The results demonstrated the feasibility of the displacement format SWNTs-based chemiresistive affinity sensor to detect small molecules with high sensitivity and selectivity and the framework presented here lays the foundation for highly efficient detection of a diverse group of analytes of interest in the fields of environmental monitoring and health care. Furthermore, the small size, facile and rapid electrical transduction mechanism, integration with modern day electronics, multi-analyte sensing using an array of sensors functionalized with different functional recognition molecules and minimum to no sample pretreatment are the many advantages of the 1-D nanostructure based label-free sensors that make them suitable for point of use/care detection. The large error bars observed in the response of our device is attributed to the batch treatment of the sensors and manual solution dispensing and can be reduced by integrating microfluidic channel for solution handling and delivery along with real-time sensing measurements. Further improvement in the performance of the sensor demonstrated in the current study is expected by applying FET-gate control and/or by fine-tuning the work function difference between the metal electrode and the conducting polymer nanowire.

## Supplementary Material

Refer to Web version on PubMed Central for supplementary material.

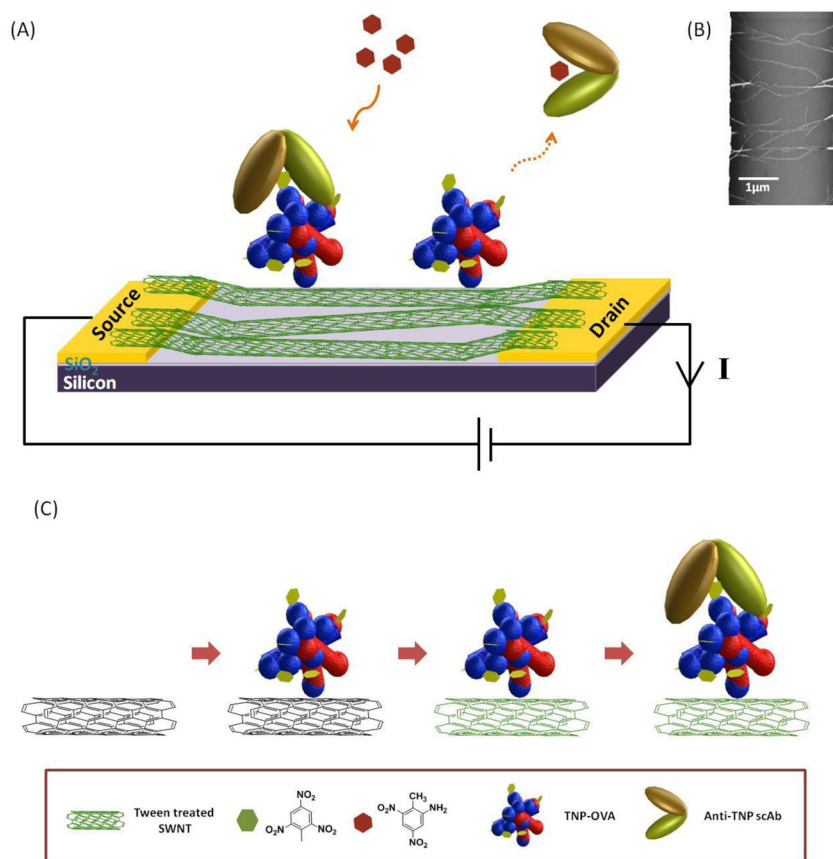
## Acknowledgments

We acknowledge the support of grants CBET-0617240 from NSF and U01ES016026 from NIH. We also would like to thank Dr. Andrew Hayhurst for providing plasmid pMoPac16.

## References

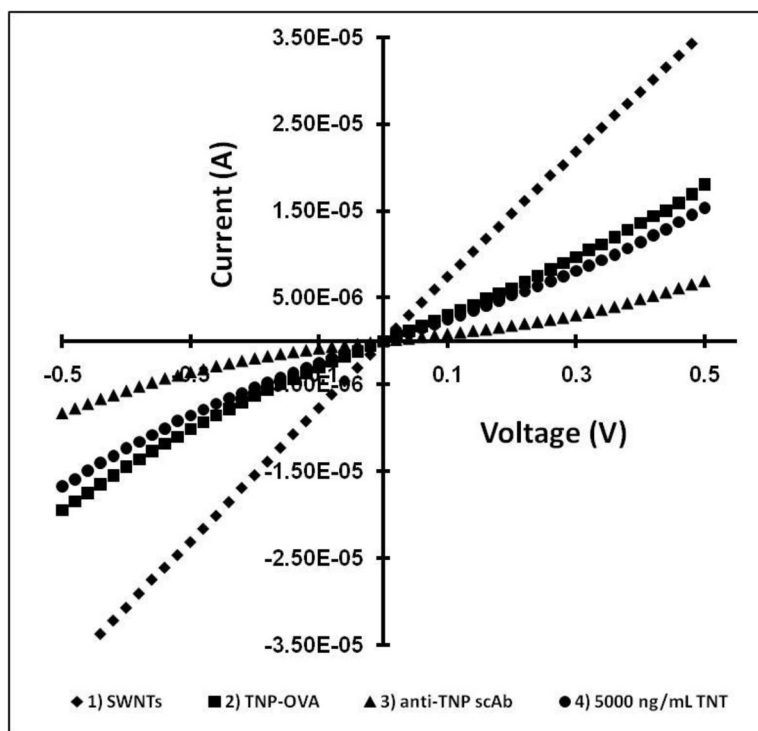
- Allen BL, Kichambare PD, Star A. *Adv Mater.* 2007; 19:1439–1451.
- Azamian BR, Davis JJ, Coleman KS, Bagshaw CB, Green MLH. *J Am Chem Soc.* 2002; 124:12664–12665. [PubMed: 12392405]
- Bangar MA, Shirale DJ, Chen W, Myung NV, Mulchandani A. *Anal Chem.* 2009; 81:2168–2175. [PubMed: 19281260]
- Elkind JL, Stimpson DI, Strong AA, Bartholomew DU, Melendez JL. *Sens Actuators, B.* 1999; 54:182–190.
- Goldman ER, Hayhurst A, Lingerfelt BM, Iverson BL, Georgiou G, Anderson GP. *J Environ Monit.* 2003; 5:380–383. [PubMed: 12833979]
- Green TM, Charles PT, Anderson GP. *Anal Biochem.* 2002; 310:36–41. [PubMed: 12413470]
- Hangarter CM, Bangar MA, Mulchandani A, Myung NV. *J Mater Chem.* 2010; 20:3131–3140.
- Halasz A, Groom C, Zhou E, Paquet L, Beaulieu C, Deschamps S, Corriveau A, Thiboutot S, Ampleman G, Dubois C, Hawari J. *J Chromatogr A.* 2002; 963:411–418. [PubMed: 12187997]
- Li C, Curreli M, Lin H, Lei B, Ishikawa FN, Datar R, Cote RJ, Thompson ME, Zhou C. *J Am Chem Soc.* 2005; 127:12484–12485. [PubMed: 16144384]
- Lim JH, Phiboolsirchit N, Mubeen S, Rheem Y, Deshusses MA, Mulchandani A, Myung NV. *Electroanalysis.* 2010; 22:99–105.
- Kim SN, Rusling JF, Papadimitrakopoulos F. *Adv Mater.* 2007; 19:3214–3228. [PubMed: 18846263]
- Larsson A, Angbrant J, Ekeröth J, Mansson P, Liedberg B. *Sens Actuators, B.* 2006; 113:730–748.
- Patolsky F, Zheng G, Lieber CM. *Nanomedicine.* 2006; 1:51–65. [PubMed: 17716209]
- Pennington JC, Brannon JM. *Thermochim Acta.* 2002; 384:163–172.

- Roberts, WC.; Commons, BJ.; Bausum, HT.; Abermathy, CO.; Murphy, JJ.; Khanna, K. Agency, USEP. 1993.
- Shankaran DR, Gobi KV, Sakai T, Matsumoto K, Toko K, Miura N. *Biosens Bioelectron.* 2005; 20:1750–1756. [PubMed: 15681190]
- Shriver-Lake LC, Breslin KA, Charles PT, Conrad DW, Golden JP, Ligler FS. *Anal Chem.* 2002; 67:2431–2435.
- Shriver-Lake LC, Donner BL, Ligler FS. *Environ Sci Technol.* 1997; 31:837–841.
- Teker K, Sirdeshmukh R, Sivakumar K, Lu S, Wickstrom E, Wang HN, Vo-Dinh T, Panchapakesan B. *Nano Bio Technology.* 2005; 1:171–182.
- Walsh ME. *Talanta.* 2001; 54:427–438. [PubMed: 18968268]
- Wanekaya AK, Chen W, Myung NV, Mulchandani A. *Electroanalysis.* 2006; 18:533–550.
- Yinon, J.; Zitrin, S. *Modern Methods and Applications in Analysis of Explosives.* Wiley; New York: 1993.

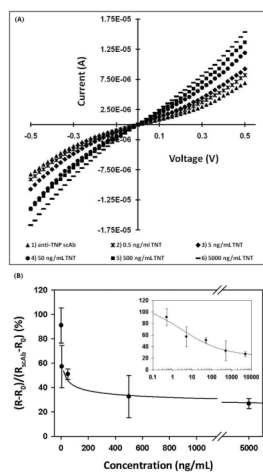


**Figure 1.** (A) Schematic diagram of the SWNT immunosensor to detect TNT. Anti-TNP scAb is leaving from the sensor platform due to displacement by TNT. (B) SEM image of aligned SWNTs between two gold electrodes. (C) Sequential modification of the sensor.

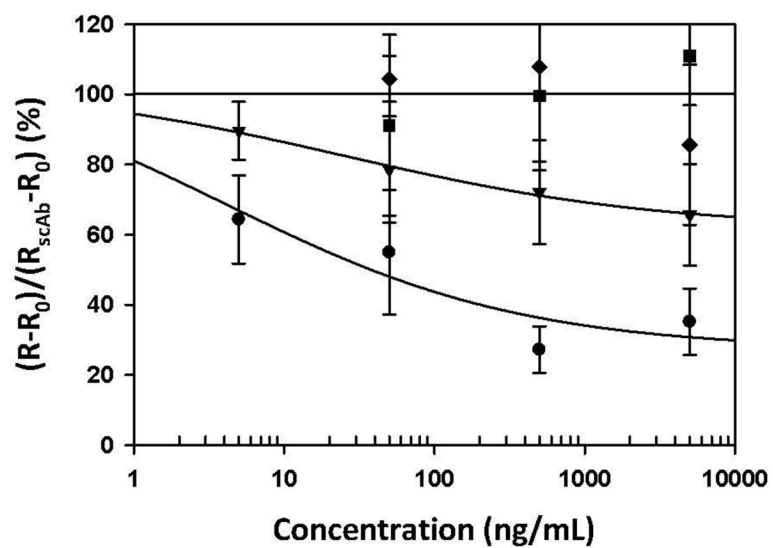




**Figure 2.** Sequential responses of the sensor during the fabrication and the sensing. When TNP-OVA was immobilized on the SWNTs, the slope of the I-V plot decreased due to accumulation of negative charge of the protein. Antibody binding to TNP on the SWNTs also led to a decrease of the slope. After adding TNT, the slope was increased back; Bare SWNTs (◆), after modification with OVA-TNP (■), incubation with anti-TNT scAb (▲), and treatment with 5000 ng/mL of TNT (●).



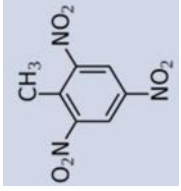
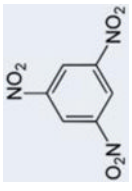
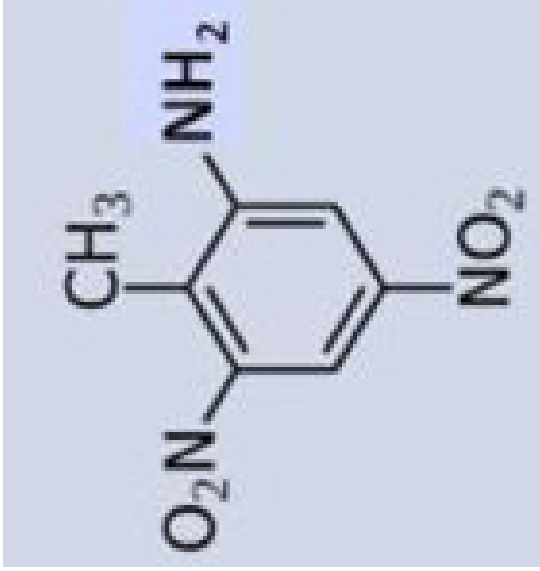
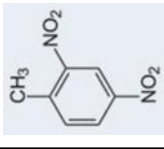
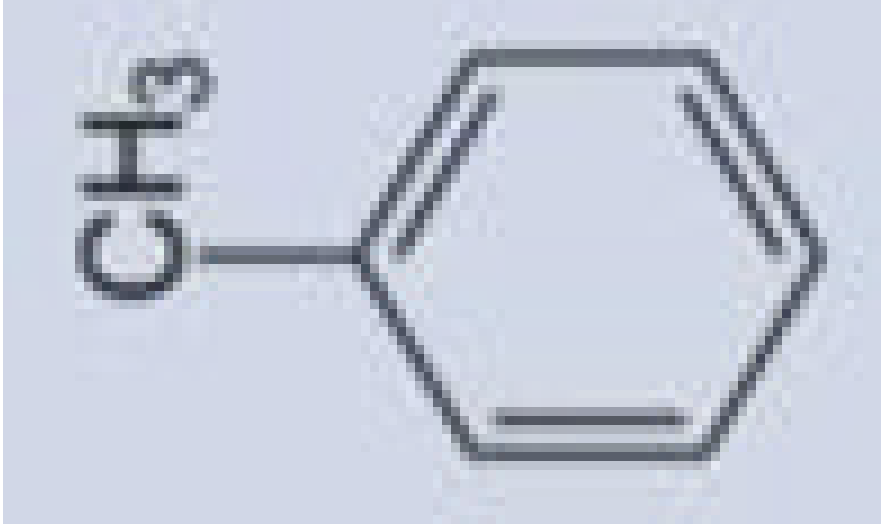
**Figure 3.** Sensor response to different concentrations of TNT; (A) I-V plot according to the each concentration of TNT; anti-TNP scAb was bound to functionalized SWNTs ( $\blacktriangle$ ), 0.5 ng/mL ( $\times$ ), 5 ng/mL ( $\blacklozenge$ ), 50 ng/mL ( $\bullet$ ), 500 ng/mL ( $\blacksquare$ ) and 5000 ng/mL ( $—$ ) of TNT were added. (B) Calibration curve of the sensor for TNT in buffer. Inset graph represents a function of the logarithm of concentration. Each data is an average of three measurements, and error bar stands for the standard deviation.



**Figure 4.** Calibration curves of the sensor for different derivatives of TNT; TNB (●), 2A-4,6-DNT (▼), 2,4-DNT (◆) and Toluene (■). Each data is an average of five measurements, and error bars stand for the standard deviation.

Table 1

IC<sub>50</sub> for TNT derivatives

Analyte Structure	<p><i>Biosens Bioelectron.</i> Author manuscript; available in PMC 2011 December 15.</p>														
TNT		TNB		2A-4,6-DNT		2,4-DNT		Toluene		IC <sub>50</sub> (ng/ml)	26	33	≥10000	Nd	Nd

**Table 2**

SWNTs Immunosensor accuracy; Values are mean of three measurements  $\pm$  standard deviation.

Spiked TNT (ng/mL)	Measured TNT (ng/mL)	Recovery (%)
0.5	0.53 $\pm$ 0.2	106.9
5	5.45 $\pm$ 1.7	109.7
50	40.30 $\pm$ 4.63	80.1